Soft matrix is a natural stimulator for cellular invasiveness

Zhizhan Gu[a,b], Fei Liu[c], Elina A. Tonkova[a], Soo Young Lee[a], Daniel J. Tschumperlin[c,d], and Michael B. Brenner[a]

[a]Division of Rheumatology, Immunology, and Allergy, Department of Medicine, Brigham and Women's Hospital, Harvard Medical School, Boston, MA 02115; [b]Department of Cancer Biology, University of Texas MD Anderson Cancer Center, Houston, TX 77054; [c]Molecular and Integrative Physiological Sciences, Department of Environmental Health, Harvard School of Public Health, Boston, MA 02115; [d]Department of Physiology and Biomedical Engineering, Mayo Clinic, Rochester, MN 55905

ABSTRACT **Directional mesenchymal cell invasion in vivo is understood to be a stimulated event and to be regulated by cytokines, chemokines, and types of extracellular matrix (ECM). Instead, by focusing on the cellular response to ECM stiffness, we found that soft ECM (low stiffness) itself is sufficient to prevent stable cell-to-cell adherens junction formation, up-regulate matrix metalloproteinase (MMP) secretion, promote MMP activity, and induce invadosome-like protrusion (ILP) formation. Consistently, similar ILP formation was also detected in a three-dimensional directional invasion assay in soft matrix. Primary human fibroblasts spontaneously form ILPs in a very narrow range of ECM stiffness (0.1–0.4 kPa), and such ILP formation is Src family kinase dependent. In contrast, spontaneous ILP formation in malignant cancer cells and fibrosarcoma cells occurs across a much wider range of ECM stiffness, and these tumor cell ILPs are also more prominent at lower stiffness. These findings suggest that ECM softness is a natural stimulator for cellular invasiveness.**

Monitoring Editor
Mark H. Ginsberg
University of California, San Diego

Received: May 16, 2013
Revised: Dec 2, 2013
Accepted: Dec 4, 2013

INTRODUCTION

Individual cell invasion falls into two categories: mesenchymal invasion and amoeboid invasion. The former requires proteolytic activity toward extracellular matrix (ECM), and the latter does not (Wolf *et al.*, 2007; Lammermann and Sixt, 2009; Friedl and Alexander, 2011). Cell invasion can be stimulated by various types of cytokines, chemokines, and ECM. Without stimulation, basal cell invasion in a three-dimensional (3D) matrix is determined by the cellular response to the matrix ligand type, density, geometry, and stiffness (Nelson *et al.*, 2006; Wolf and Friedl, 2011). To simplify and dissect basal invasion, here we focus on how cell invasion is regulated selectively by substrate stiffness under conditions in which the ECM type and ligand density are constant.

Amoeboid invasion uses Rac-dependent filapodia or Rho-dominated blebbing to help cells penetrate, stretch, and squeeze through the ECM to reach a distal docking ligand so as to pull the trailing cell body forward (Friedl *et al.*, 2001; Lorentzen *et al.*, 2011; Poincloux *et al.*, 2011). For amoeboid cell invasion, the ECM has to be either porous enough for a cell to squeeze in or "soft" enough for a cell to penetrate through. However, it is largely unknown how ECM stiffness/softness regulates mesenchymal-type cell invasion.

RESULTS

Soft matrix prevents stable cell-to-cell adherens junction formation

Cells can respond to the stiffness of their surrounding matrices (Discher *et al.*, 2005). A simplified model of two-dimensional (2D) cell culture has been developed to investigate the cell response to ECM stiffness without changing ECM ligand type, density, or geometry (Pelham and Wang, 1997; Liu *et al.*, 2010; Myers *et al.*, 2011).

This article was published online ahead of print in MBoC in Press (http://www.molbiolcell.org/cgi/doi/10.1091/mbc.E13-05-0260) on December 11, 2013.

Z.G. raised the hypothesis, designed the project, performed the experiments, and wrote the manuscript. F.L. helped make stiffness gels, performed the MMP activity experiment, and provided helpful comments. E.A.T. and S.Y.L. helped with the experiments. D.J.T. provided collaboration and helpful comments and contributed to the writing of the manuscript. M.B.B. supervised all aspects of the project and contributed to writing the manuscript.

Address correspondence to: Michael B. Brenner (mbrenner@research.bwh.harvard.edu), Zhizhan Gu (zhizhan.gu@alumni.brown.edu).

Abbreviations used: AJ, adherens junction; ECM, extracellular matrix; FAK, focal adhesion kinase; FLP, filopodium-like protrusion; ILP, invadosome-like protrusion; MMP, matrix metalloproteinase; SFK, Src family kinase; TIMP, tissue inhibitor of metalloproteinase.

By using such cell culture systems, we fine-tuned ECM stiffness from the gigapascal range of glass and plastic, traditional in vitro cell culture, down to 0.1 kPa. The basal stiffness of soft tissues such as lymph node, liver, and lung ranges from ~0.1 to ~20 kPa (Discher *et al.*, 2005; Hinz, 2007; Janmey and McCulloch, 2007). Similar to cells cultured on glass and plastic, primary human fibroblasts cultured for 24 h on the ECM substrates with stiffness >6.4 kPa display classic fibroblast morphology, with mesenchymal cadherin-11 clustering in adherens junctions (AJs; Valencia *et al.*, 2004; Lee *et al.*, 2007), as well as long actin stress fibers (Gu *et al.*, 2011). Strikingly, fibroblasts grown on gels of 0.2-kPa stiffness lost both AJs and well-organized long actin stress fibers, regardless of cell density (Figure 1A and Supplemental Figure S1A). The loss of AJ formation on gels of 0.2-kPa stiffness was further confirmed by staining the p120 catenin, an AJ structural component protein (Figure 1B). The total amount of cadherin and catenin proteins in these cells on substrates with varying stiffness remained stable (Figure 1C). To initiate individual cell invasion, cells in tissue must break adhesion interactions with neighboring cells (Friedl and Alexander, 2011). Such loss of cell-to-cell adhesion suggests a cell migration/invasion phenotype.

Soft matrix up-regulates matrix metalloproteinase secretion and promotes matrix metalloproteinase activity

Matrix metalloproteinases (MMPs) are critical proteinases in ECM degradation and include two major subfamilies of secreted MMPs (MMP-2, -3, etc.) and integral membrane MMPs (MMP-14 [MT1-MMP], -15, etc.; Kessenbrock *et al.*, 2010). For all types of MMPs that were measured, increased ECM stiffness significantly inhibited MMP secretion from these cells (Figure 2A). Previous studies reported that increased ECM stiffness significantly promotes primary cell proliferation (Wang *et al.*, 2000; Liu *et al.*, 2010). Thus, by normalizing to total cell numbers at 48 h after cell seeding, the relative amount of MMPs secreted per cell were even lower on stiffer substrates (Figure 2B). Further, the total MMP activities of these secreted MMPs also were higher on softer substrates and lower on stiffer substrates (Figure 2C). Of interest, we also detected small differences of MMP secretion on substrates with varying stiffness as early as 4 h after cell seeding (Supplemental Figure S1B), suggesting that cells begin responding to stiffness during their initial adhesion to ECM. To determine whether MMP secretion correlated with actual ECM degradation, we used an MMP ECM degradation functional assay using DQ collagens that were evenly cross-linked to substrates with varying stiffness. DQ collagens have no fluorescence in their intact form but emit strong fluorescence upon degradation by MMPs or other proteinases. Using this sensitive assay, we noted a substantial DQ collagen degradation difference as early as 4 h after cell seeding onto substrates of varying stiffness. Maximal DQ collagen degradation by cells was detected on the gels of 0.2-kPa stiffness, intermediate degradation was noted on the gels of 25.6-kPa stiffness, but only minimal DQ collagen degradation was detected on glass (Figure 3A). Fluorescence intensity quantitation shows DQ collagen degradation per cell on gels of 0.2-kPa stiffness was nearly fivefold that on 25.6-kPa gels and more than eightfold that on glass (Figure 3B). Tissue inhibitor of metalloproteinase-1 (TIMP-1) preferentially inhibits secreted MMPs, as well as MT4-MMP and MT6-MMP, but not other membrane-type MMPs, such as MMP-14 (MT1-MMP). In contrast, TIMP-2 and batimastat inhibit both secreted and membrane-type MMPs (Nagase *et al.*, 2006; Sabeh *et al.*, 2009). In our DQ collagen assay, both TIMP-2 and batimastat significantly inhibited DQ collagen degradation by cells on the gels of 0.2-kPa stiffness. TIMP-1 partially inhibited such degradation (Figure 3, A and B). These results suggest that not only secreted MMPs, but also membrane-type MMPs contribute to the ECM degradation during the early stage of cell adhesion to the soft ECM.

Soft matrix induces invadosome-like protrusion formation

Next we examined cell morphology to determine whether changes consistent with cell invasion were influenced by ECM stiffness. We stained F-actin in human primary fibroblasts at 4 h of cell adhesion to the ECM substrates of varying stiffness, ranging from gigapascals on glass down to 0.1 kPa. Strikingly, for all cells cultured on the ECM substrates with stiffness >6.4 kPa, F-actin morphology was similar to that of the classic long F-actin stress fibers in normal primary fibroblasts traditionally cultured on glass or plastic tissue culture plates (Gu *et al.*, 2011). Of interest, by reducing stiffness to 0.4 kPa, the fibroblasts formed fewer, shorter, and thinner F-actin fibers. Remarkably, at 0.2 kPa, these cells lost almost all short F-actin fibers. Instead, F-actins formed large and condensed clusters in these cells (Figure 4A). Such dramatic cytoskeletal morphology changes drew our attention to costaining the major membrane-type MMP-14 in these cells together with F-actin and cell-to-matrix adhesion molecule integrin β1. In all cells cultured at 6.4-kPa and higher stiffness, integrin β1 clustered at the tips of F-actin stress fibers to form classic focal adhesions as seen in fibroblasts cultured on glass or plastic tissue culture plates (Gu *et al.*, 2011). MMP-14 showed the expected pattern of intracellular clusters at the perinuclear endocytic-recycling compartment (Williams and Coppolino, 2011). MMP-14 did not show a strong fluorescence signal at the cell surface, as it was evenly distributed on the cell surface, and the weak homogeneous fluorescence signal was subtracted by the confocal microscope offset settings. Of interest, cells on gels of 0.4-kPa stiffness formed much smaller integrin β1 focal adhesions on the tips of fewer, shorter, and thinner F-actin fibers, whereas MMP-14 morphology did not dramatically change in comparison to cells on gels of 6.4-kPa stiffness. In contrast, for cells on gels of 0.2-kPa stiffness, MMP-14 formed large clusters on the cell surface and colocalized with the F-actin clusters in these cells. Meanwhile, cell surface integrin β1 localized in small clusters in and around these large MMP-14– and F-actin–positive clusters (Figure 4B). This morphology, including MMP-14, F-actin, and integrin β1, is similar to the newly defined cell invasion structures called invadosomes (invadopodia and podosomes) that are found in highly invasive cells (Buccione *et al.*, 2004; Linder, 2009). Note that these previously reported examples of invadosomes were observed in traditional in vitro cell culture conditions on plastic or glass. Invadosomes usually have a round actin core and situate behind the plasma membrane borderline from an *xy* view on traditional 2D culture surfaces. In comparison, the clusters we found on the gels of 0.2-kPa stiffness situate at the tip of the plasma membrane. They stretch outward and have shapes more like the filopodium-like protrusions (FLPs) found in invasive cancer cells in 3D cultures (Shibue *et al.*, 2012). However, due to limited characterization of recently reported FLPs and lack of information regarding MMP-14 clustering in FLP structures, here we term these clusters on gels of 0.2-kPa stiffness as invadosome-like protrusions (ILPs; Carman, 2009).

Zoom-in and 3D confocal microscopy showed such MMP-14 and F-actin clusters in cells on gels of 0.2-kPa stiffness displayed columnar structures on the *z*-axis that are perpendicular to the stiffness gel surface (Figure 4C). These MMP-14 clusters were confirmed to be on the cell surface by staining the MMP-14 extracellular hinge region domain without membrane permeabilization (Figure 4D). Meanwhile, another invadosome marker protein, cortactin, colocalized perfectly with MMP-14 and F-actin at these structures (Figure 5A). Further, in situ invadosome zymography assays showed ECM degradation at these structures in cells on gels of 0.2-kPa stiffness, whereas

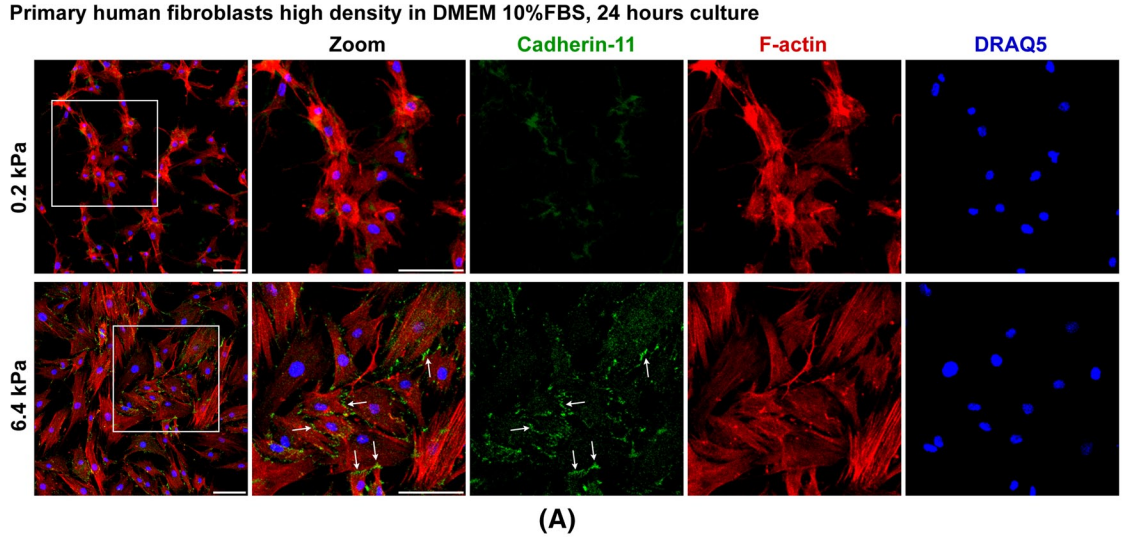

(A)

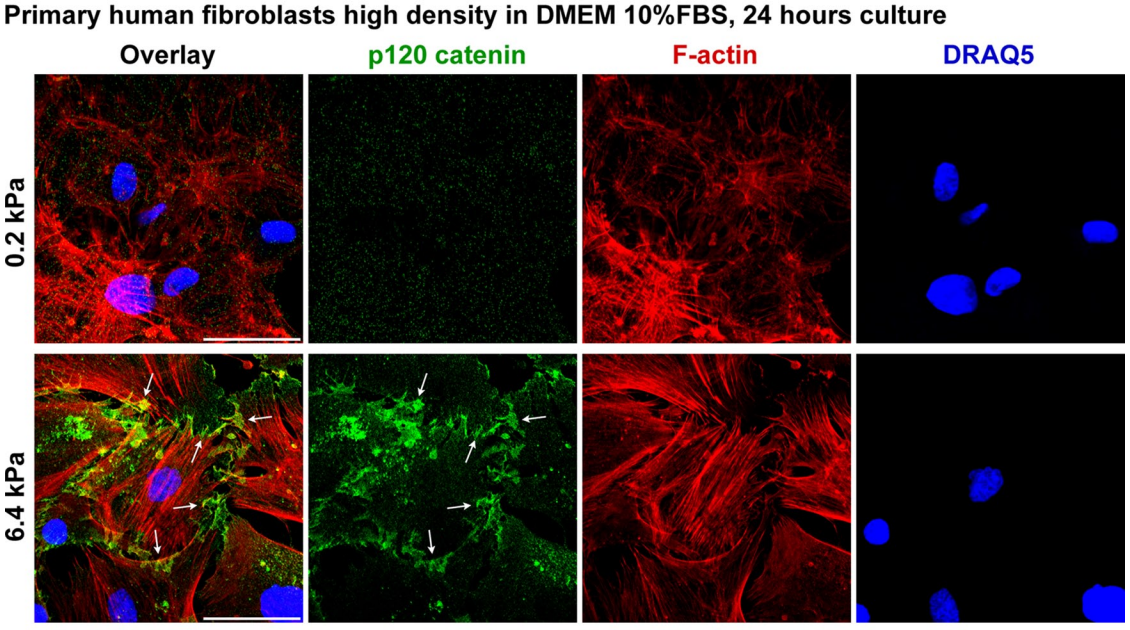

(B)

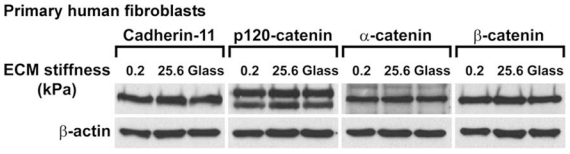

(C)

FIGURE 1: ECM softness prevents AJ formation. (A) Primary human fibroblasts (3×10^4 cells per well) were seeded onto gels of varying stiffness in 12-well plates and cultured for 24 h. Cell surface cadherin-11 was live stained by monoclonal anti–cadherin-11 (3H10) antibody for 1 h at room temperature, followed by fixation and secondary antibody staining. Plasma membranes were then permeabilized, and intracellular F-actins were stained by phalloidin. Cell nuclei were stained by DRAQ5. Arrows point to cadherin-11 adherens junctions. Scale bar, 100 μm. (B) Primary human fibroblasts (3×10^4 cells per well) were seeded onto gels of varying stiffness in 12-well plates and cultured for 24 h. Cells were then fixed, and cell membranes were permeabilized. p120 catenin was stained by monoclonal anti–p120 catenin antibody. Arrows point to p120 catenin–positive adherens junctions. Scale bar, 50 μm. (C) Primary human fibroblasts were cultured as in A, and total cell lysates were subject to SDS–PAGE and Western blot for cadherin-11, p120-catenin, α-catenin, and β-catenin. β-Actin as protein loading control.

cells on gels of 6.4-kPa stiffness did not form such structure to degrade ECM (Figure 5B, top). The ECM degradation at the center of these cells on gels of 0.2-kPa stiffness was most likely performed by secreted MMPs, which is consistent with our previous findings (Supplemental Figure S1B). A 3D-to-2D *xz*-axis maximum projection showed these ILPs formed on gels of 0.2-kPa stiffness invaded into

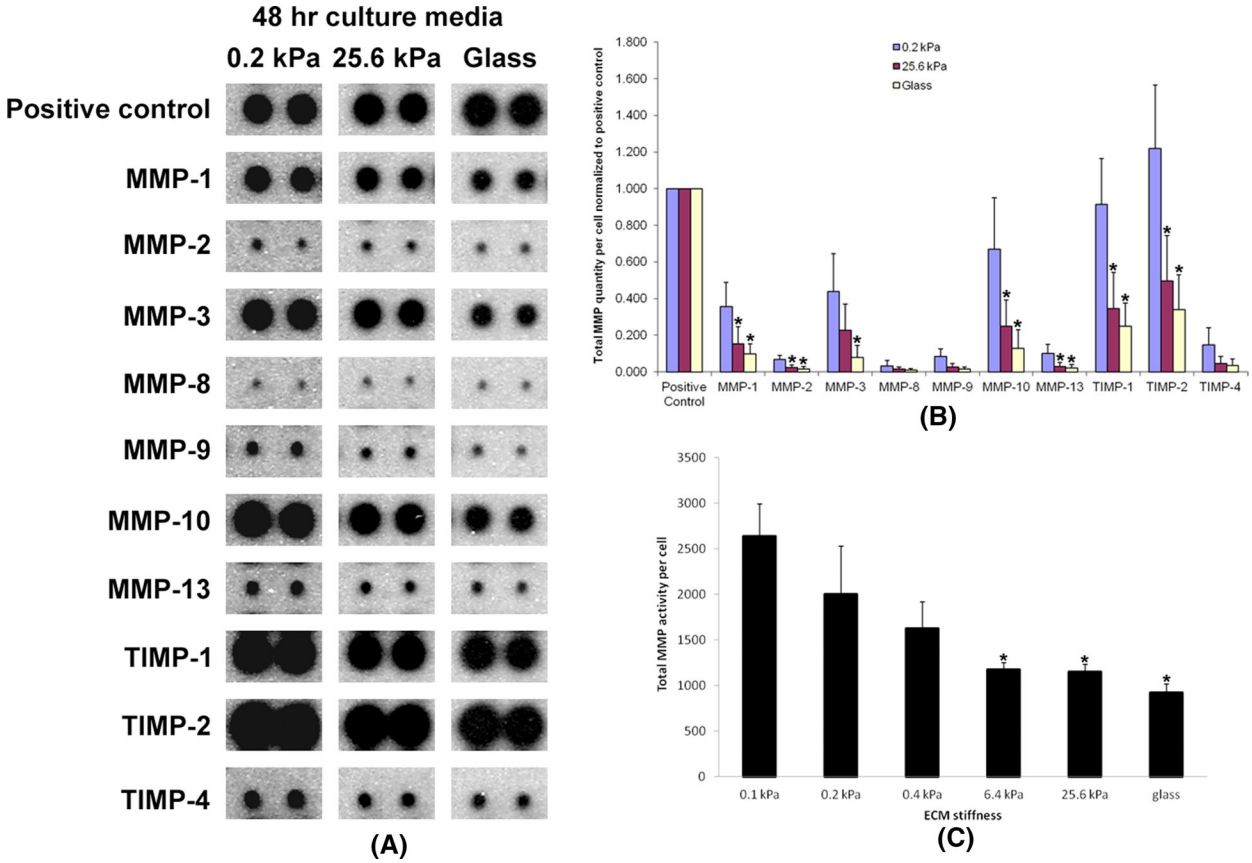

FIGURE 2: ECM softness upregulates MMP secretion and promotes MMP activity. (A) Primary human fibroblasts (2×10^4 cells per well) were seeded onto gels of varying stiffness in 12-well plates and cultured for 48 h. Cell culture medium from each condition was collected and subject to the RayBio Human MMP Array to determine the total secreted MMP protein quantity in each medium. (B) Three independent experiments ($n = 3$, ±SD) as in A were performed and quantified. Note that proliferation rates vary on gels of different stiffness . Total MMP quantities were normalized to total cell numbers on gels of varying stiffness at 48 h. Student's *t* test was used for the comparison of each mean with the mean of MMP protein quantity of the same MMP type on 0.2-kPa gels. *$p < 0.05$ considered significant. (C) Cell culture conditioned media were collected as in A, and the total MMP activity in each medium was measured and quantified ($n = 3$, ±SD) and normalized to cell number. Student's *t* test was used for the comparison of each mean with the mean of "0.1 kPa." *$p < 0.05$ considered significant.

the fluorescent ECM on top of the stiffness gels underneath (Figure 5B, bottom). All these characteristics of such MMP-14–containing structures in cells on gels of 0.2-kPa stiffness fulfilled the criteria for ILPs (Buccione *et al.*, 2004; Carman, 2009; Linder, 2009). These findings led us to propose that soft ECM itself is sufficient to induce spontaneous ILP formation in primary human fibroblasts. Indeed, fibroblasts have long been defined as mesenchymal invasive cells (Bhowmick *et al.*, 2004; Gaggioli *et al.*, 2007). However, previously invadosomes were reported in macrophages, cancer cells, and Src-transformed fibroblast cell lines but not in normal primary fibroblasts (Mizutani *et al.*, 2002; Bharti *et al.*, 2007). These data now reveal that normal primary fibroblasts can spontaneously form ILPs on soft ECM but not on stiff surfaces such as glass or plastic tissue culture plates. As a control, we switched from collagen-coated stiffness gels to fibronectin-coated stiffness gels and also saw similar ILP formation on these soft matrices (Supplemental Figure S1C). These results suggest that such ILP formation is particularly stiffness but not matrix type dependent. Of interest, serum in the media is essential for ILP formation on gels of 0.2-kPa stiffness regardless of whether they are collagen or fibronectin coated (unpublished data).

Next we determined the time frame of ILP formation on gels of 0.2-kPa stiffness. About 30% of the primary fibroblasts began forming ILPs as early as 1 h after cell seeding, and ILP formation peaked at 4 h. After that, some fibroblasts started to lose ILPs over time and displayed a long, linear cell shape (Supplemental Figure S2, A and B). Thus spontaneous ILP formation in these normal primary fibroblasts is induced by matrix softness during the initial stage of cell adhesion to ECM. The loss of ILPs over time occurs possibly because fibroblasts can remodel ECM and change the surrounding ECM properties, including stiffness over time (see later discussion of Figure 9B; Jodele *et al.*, 2006; Neilson, 2006).

Soft matrix–induced ILP formation is Src family kinase dependent

Src is a nonreceptor tyrosine kinase that associates with integrins and focal adhesion kinase (FAK) to regulate cell adhesion (Zachary and Rozengurt, 1992; Parsons and Parsons, 1997). Previously invadosome formation in fibroblasts cultured on stiff surfaces such as glass was only studied in Src-transformed fibroblasts. Further, Src has been reported to regulate invadosome formation in many other cell types (Hauck *et al.*, 2002; Bharti *et al.*, 2007). Of interest, recent studies suggest that not only Src, but also Src family kinases (SFKs), are invadosome-formation regulators (Ayala *et al.*, 2008; Enomoto *et al.*, 2009). Thus we quantitated SFK activity over time during ILP

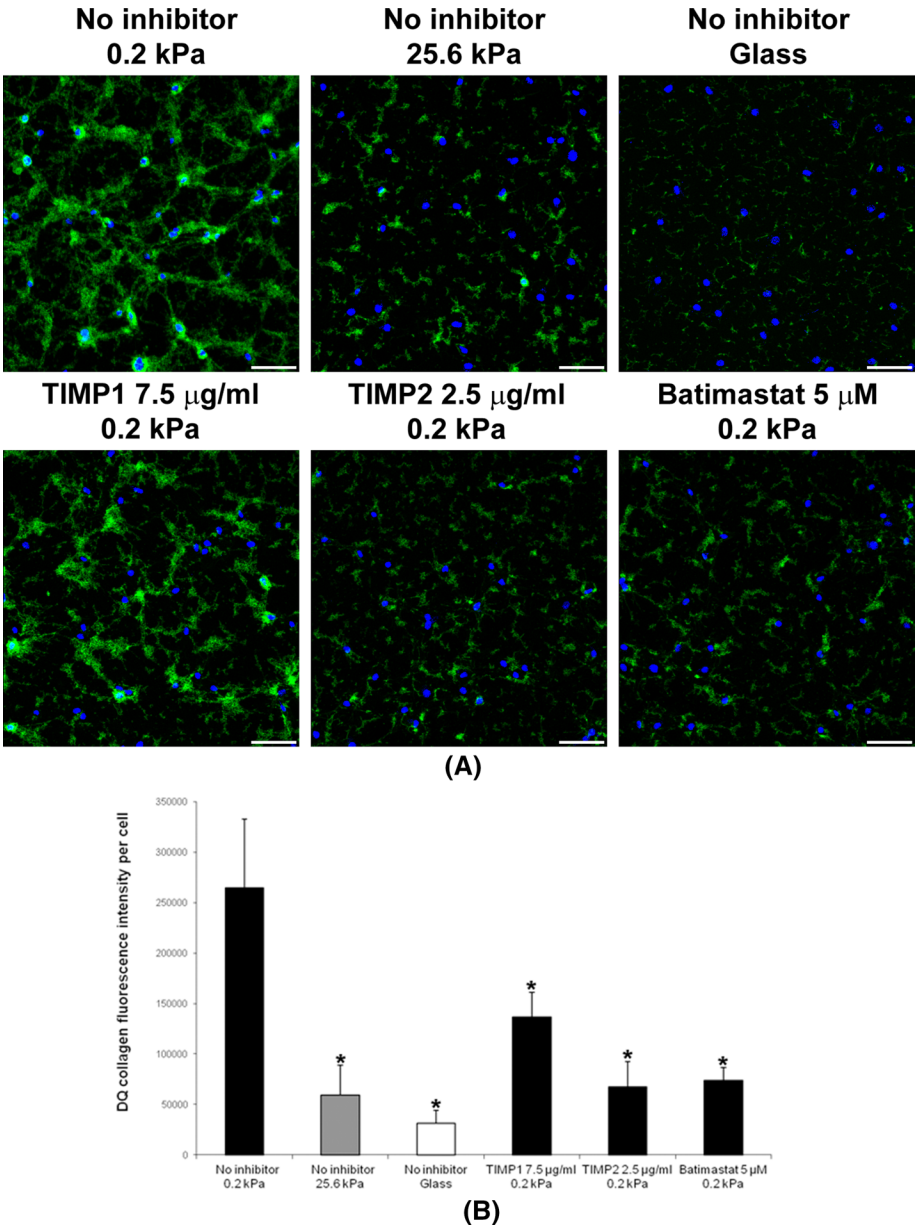

FIGURE 3: ECM softness stimulates matrix degradation. (A) DQ collagens were cross-linked onto gels of varying stiffness. Primary human fibroblasts (2×10^4 cells per well) were seeded onto gels of varying stiffness in 12-well plates and cultured for 4 h with or without MMP inhibitors. Cell nuclei were stained by DRAQ5. Green fluorescence indicated cleaved DQ collagen. Scale bar, 100 μm. (B) Five independent experiments ($n = 5$, ±SD) as in A were performed, and the fluorescence intensities of DQ collagens in these images were measured, quantified, and normalized to number of cells. Student's *t* test was used for the comparison of each mean with the mean of "No inhibitor 0.2 kPa." *$p < 0.05$ considered significant.

formation in normal primary fibroblasts on substrates with varying stiffness by using an anti–phospho-Src (pY418) antibody that recognizes all activated SFKs (Oneyama *et al.*, 2008; Enomoto *et al.*, 2009). Strikingly, SFK phosphorylation was turned on early, maintained, and raised during cell adhesion on soft (0.2-kPa stiffness) gels. However, on gels of 25.6-kPa stiffness, although SFK phosphorylation was turned on early, it gradually decreased over time. On the rigid glass surface, SFK phosphorylation was only weakly and transiently turned on during cell adhesion (Figure 6, A and B). Specific SFK inhibition by SU6656 or Dasatinib significantly blocked ILP formation and cell spreading in primary fibroblasts on gels of 0.2-kPa stiffness. Such SFK inhibition only partially blocked focal adhesion formation and cell spreading in cells on gels of 6.4-kPa stiffness (Figure 6, C and D, and Supplemental Figure S2C), since SFK also regulates integrin focal adhesion formation (Zachary and Rozengurt, 1992; Parsons and Parsons, 1997).

Further phosphokinase antibody array analyses revealed that Pyk2 and SFKs, including Src, Fyn, Hck, Lyn, and Yes but not Lck or Fgr, were significantly activated at the 4-h time point of cell adhesions on gels of 0.2-kPa stiffness (Supplemental Figure S3A), which is the time point at which ILP formation peaked on such soft gels (Supplemental Figure S2, A and B). In comparison, these SFKs were less activated at the same time point of cell adhesion onto the stiffer matrices of 25.6-kPa gels or glass (Supplemental Figure S3A). It will be important to understand the roles of SFK regulators such as RPTPalpha (Jiang *et al.*, 1999) and CSK (Nada *et al.*, 1991; Superti-Furga *et al.*, 1993) and SFK downstream effectors such as Grb2 (Yamaguchi *et al.*, 2005; Murphy and Courtneidge, 2011), Tks4 (Buschman *et al.*, 2009; Gianni *et al.*, 2009), and Tks5 (Diaz *et al.*, 2009) during such ILP formation on soft matrix.

Of interest, when ILP formation peaked on gels of 0.2 kPa stiffness (4-h time point of cell adhesions), paxillin but not FAK was significantly activated (Supplemental Figure S3B), which is consistent with previous findings that paxillin is phosphorylated during invadopodia formation (Badowski *et al.*, 2008) and FAK depletion actually switches focal adhesion formation to invadopodia formation (Chan *et al.*, 2009). We also detected that Akt, MEK 1/2, ERK 1/2, p38α, and JNK proteins were significantly phosphorylated at the time point at which these ILP formation peaked on gels of 0.2-kPa stiffness (4-h time point of cell adhesions; Supplemental Figure S3, C and D). These signaling pathway results are consistent with previous findings on the invadopodia formation signaling pathway (Schwartz *et al.*, 1995; Duong *et al.*, 1998; Furmaniak-Kazmierczak *et al.*, 2007; Gil-Henn *et al.*, 2007; Magalhaes *et al.*, 2011; Yamaguchi *et al.*, 2011; Pignatelli *et al.*, 2012) and further support that on gels of 0.2-kPa stiffness, these cell surface adhesion structures containing colocalized MMP-14, cortactins, and actins are ILPs (Figures 4 and 5).

Primary fibroblasts form ILPs in a narrow range of ECM stiffness, but ILP formation in malignant cells occurs across a wide range of ECM stiffness

To determine whether ECM softness induced spontaneous ILP formation is general for primary cells of various tissues, we compared normal human fibroblasts from synovium, skin (Hs27), and lung (LL

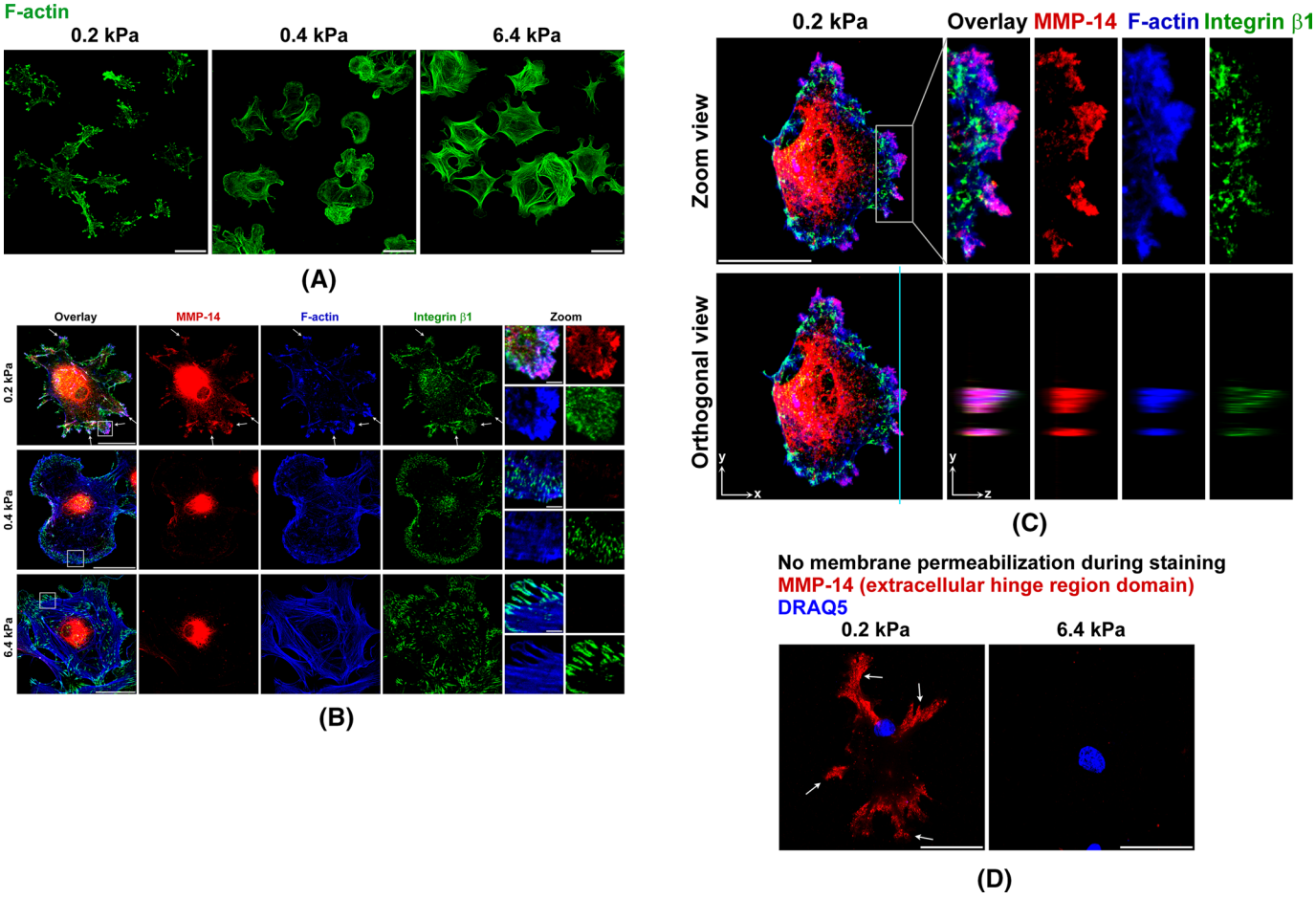

FIGURE 4: ECM softness induces spontaneous ILP formation. (A–C) Primary human fibroblasts were seeded onto gels of varying stiffness and cultured for 4 h. Cells were then fixed, and cell membranes were permeabilized for immunofluorescence (IF) staining. MMP-14 and integrin β1 were stained by primary antibodies, followed by fluorescent secondary antibodies. F-actin was stained by phalloidin–Alexa 647. All 2D images were projected from relevant confocal 3D stacks by the maximum projection method. Scale bar, 100 μm; in zoom panels, 10 μm. Arrows point to ILPs. (A) F-actin was stained by phalloidin–Alexa 647 and was defined as green color. (C) Top, zoom views of ILPs. Bottom, *z*-axis orthogonal views of ILPs showing their classic columnar shapes. The *z*-axis distances are 5× exaggerated. The vertical line defines the orthogonal view position. (D) Primary human fibroblasts were seeded onto gels of varying stiffness and cultured for 4 h. Cells were then fixed, but with no cell membrane permeabilization before IF staining. MMP-14 was stained by a primary antibody that specifically recognizes the MMP-14 extracellular hinge region domain. Cell nuclei were stained by DRAQ5. All 2D images were projected from relevant confocal 3D stacks by the maximum projection method. Scale bar, 100 μm.

24), normal human endothelial cells (HUV-VE-C), two examples of invasive human breast cancer cells (MDA-MB-231 and BT549), and two examples of invasive human fibrosarcoma cells (HS 93.T and HS913T). For all cells tested, the number of cells forming ILPs decreased when ECM stiffness increased. Thus ECM softness induces spontaneous ILP formation in all cell types. However, for all normal human fibroblasts and endothelial cells, spontaneous ILP formation was restricted to a very narrow range of ECM stiffness, 0.1–0.4 kPa. In contrast, for all malignant cancer cells and fibrosarcoma cells, spontaneous ILP formation occurred over a much wider range of ECM stiffness. For example, ~30% of the MDA-MB-231 breast cancer cells still spontaneously formed ILPs on glass (Figures 7, A and B, and 8, A and B, and Supplemental Figure S4, A and B). These results suggest that, for normal fibroblasts or endothelial cells, a slight decrease of ECM stiffness of tissue can induce their invasion, whereas a slight increase of ECM stiffness can quickly shut down their invasion. However, for cancer cells or fibrosarcoma cells, many of these cells can invade regardless of ECM stiffness, which is consistent with previous findings that some cancer cell lines can form invadosomes on gels of very rigid stiffness (Parekh *et al.*, 2011).

Similar ILP formation is detected in cells cultured in soft 3D matrices

Finally, we were interested in whether we could find the ILPs that we observed on soft 2D stiffness gels during real-time cell invasion in soft 3D matrices. We developed a directional cell invasion assay in which we could use four-dimensional (4D; three space dimensions plus time) confocal live-cell imaging to trace real-time cell invasion in 3D matrices (Supplemental Figure S5). During 16-h directional cell invasion in this assay, these human primary fibroblasts invaded 300 μm in distance (Figure 9A and Supplemental Video S1). During this invasion through the 3D soft matrix, high-magnification, small-pinhole confocal microscopy detected that every single primary fibroblast formed several invasive protrusions that looked similar to

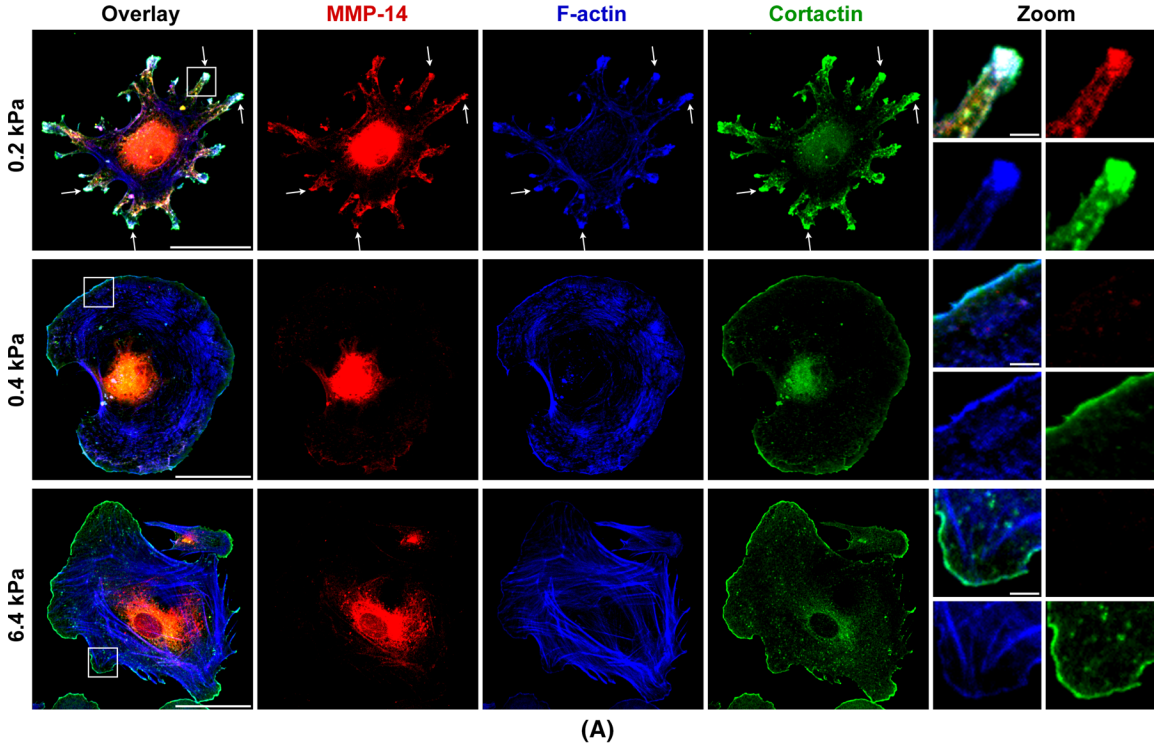

(A)

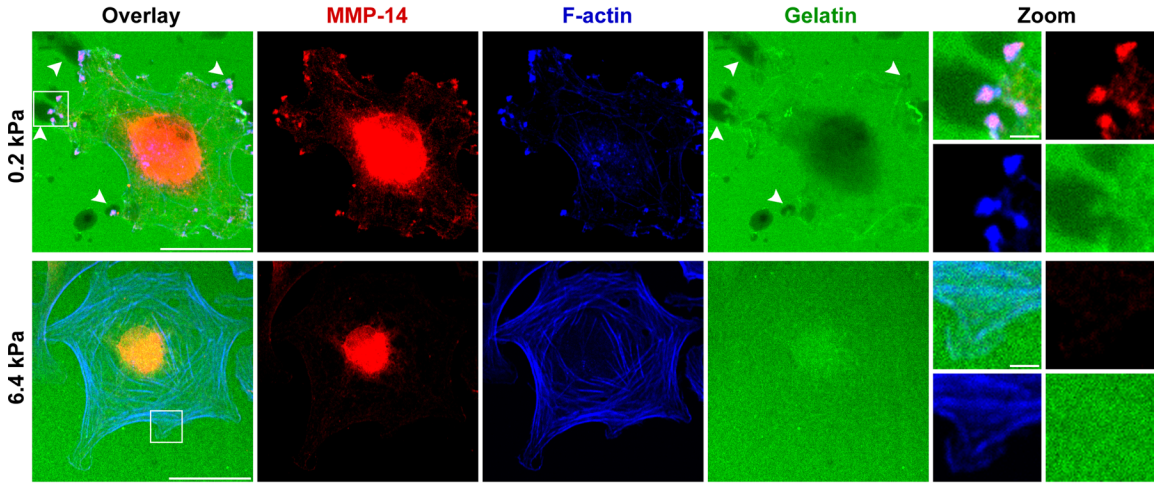

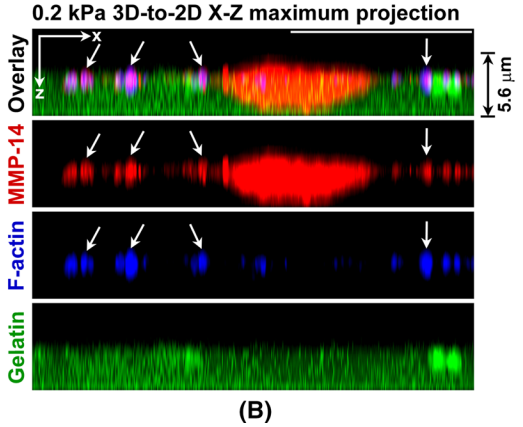

(B)

FIGURE 5: ECM softness induces spontaneous ILP formation. (A) Cells were prepared as in Figure 4B. MMP-14 and cortactin were stained by primary antibodies and followed by fluorescent secondary antibodies. F-actin was stained by phalloidin–Alexa 647. All 2D images were projected from relevant confocal 3D stacks by maximum projection method. Scale bar, 100 μm; in zoom panels, 10 μm. Arrows point to ILPs. (B) Gelatin–Oregon 488 was cross-linked to stiffness gels before cell seeding. Black areas represent degraded gelatins. Arrows point to ILPs.

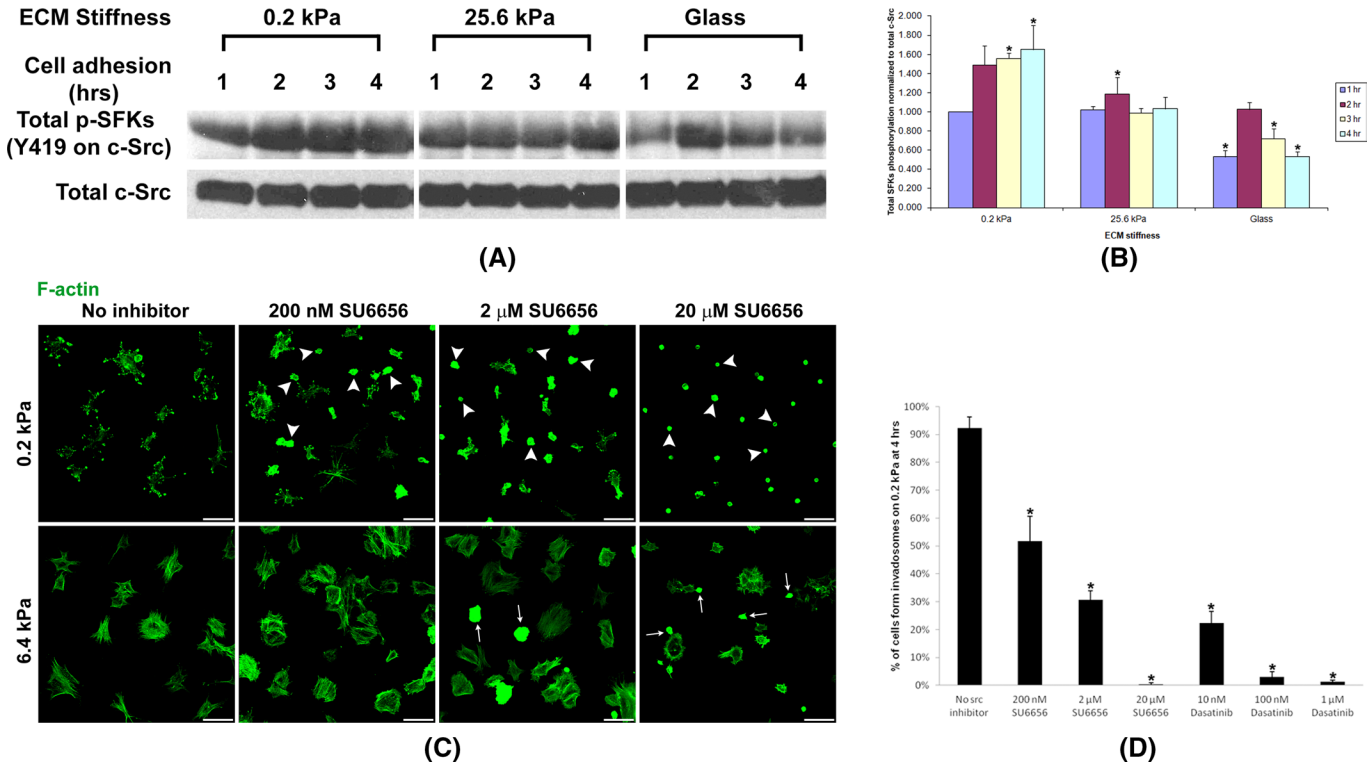

FIGURE 6: ECM softness–induced ILP formation is SFK dependent. (A) Primary human fibroblasts were seeded onto gels of varying stiffness and cultured for the hours indicated. Total cell lysates were subject to SDS–PAGE and Western blot for phospho-SFK (Y419 on c-Src). The anti–phospho-Src (pY419) antibody recognizes all activated SFKs. Total c-Src as protein loading control. (B) Three independent experiments ($n = 3$, ±SD) as in A were performed, and phospho-SFK Western blot band intensities were quantified. Student's *t* test was used for the comparison of each mean with the mean of SFK phosphorylation at 1 h on 0.2-kPa gels. *$p < 0.05$ considered significant. (C) Primary human fibroblasts were seeded onto gels of varying stiffness and cultured for 4 h with or without SFK inhibitors. Top, arrowheads point to cells unable to form ILPs upon SFK inhibition on gels of 0.2-kPa stiffness. Bottom, arrows point to cells unable to form stress fibers upon SFK inhibition on gels of 6.4-kPa stiffness. Scale bar, 100 μm. (D) Three independent experiments ($n = 3$, ±SD) as in C and Supplemental Figure S2C were performed, and the percentage of cells forming ILPs on gels of 0.2-kPa stiffness was quantified. In each experiment, 200 cells in total were counted. Student's *t* test was used for the comparison of each mean with the mean of "No src inhibitor." *$p < 0.05$ considered significant.

the ILPs that we observed on soft 2D stiffness gels (Figure 9B vs. Figures 4 and 5). Of interest, we also found that these fibroblasts largely remodeled their surrounding matrices during 3D invasion (Figure 9B, gelatin panels), which is similar to a previous finding that fibroblasts make tunnels in 3D soft matrix during invasion (Gaggioli *et al.*, 2007).

DISCUSSION

We found that soft ECM 1) prevents stable cell-to-cell adherens junction formation, 2) up-regulates MMP secretion, 3) promotes MMP activity, and 4) induces ILP formation (Figure 9C). These findings suggest that ECM softness itself is sufficient to promote cellular invasiveness even without additional stimulation from cytokines or chemokines in vivo. However, 3D mesenchymal cell invasion is a complicated process of 2D cell migration (focal adhesion–based cell-to-matrix attachments, etc.) plus cell-matrix proteolysis (invadosome formation and MMP secretion, etc.; Wolf *et al.*, 2007; Wolf and Friedl, 2011). Other laboratories report that stiffer substrate actually promotes focal adhesion–based 2D cell migration (Zaman *et al.*, 2006; Levental *et al.*, 2009; Liu *et al.*, 2010; Pathak and Kumar, 2012). Our results indicate that increased matrix stiffness is negatively correlated with cell-matrix proteolysis while being positively correlated with cell-matrix adhesion. Thus we hypothesize that the optimal matrix stiffness–regulated 3D mesenchymal cell invasion may represent the intersection of the stiffness cell-matrix "proteolysis" curve and the stiffness cell-matrix "adhesion" curve (Figure 9D). According to our findings in stiffness-regulated ILP formation, the stiffness cell-matrix proteolysis curves of normal cells are distinct from those of malignant cells (Figure 8B).

We showed, for the first time, that normal cells can spontaneously form ILPs in response to a very narrow range of soft ECM stiffness, suggesting that normal cells are largely kept quiescent from invasion by surrounding tissue stiffness. Even a modest reduction in normal soft tissue stiffness could prompt enhanced matrix invasion. Thus, when the surrounding tissue stiffness decreases, quiescent normal cells (such as fibroblasts and endothelial cells) may be activated for invasion. For example, during the early stages of wound healing, the decrease of matrix density and stiffness due to injury and/or fluid infiltration readily encourages fibroblast local invasion into the wounded site until a point at which physiologically appropriate matrix density and stiffness are rebuilt.

In contrast, malignant cells can form ILPs across a wide range of ECM stiffness. Some cancer cells can even form ILPs on superhard surfaces such as glass or plastic, suggesting that they are intrinsically invasion active and can overcome the surrounding tissue stiffness inhibition of cell invasion (Parekh *et al.*, 2011). However, both the

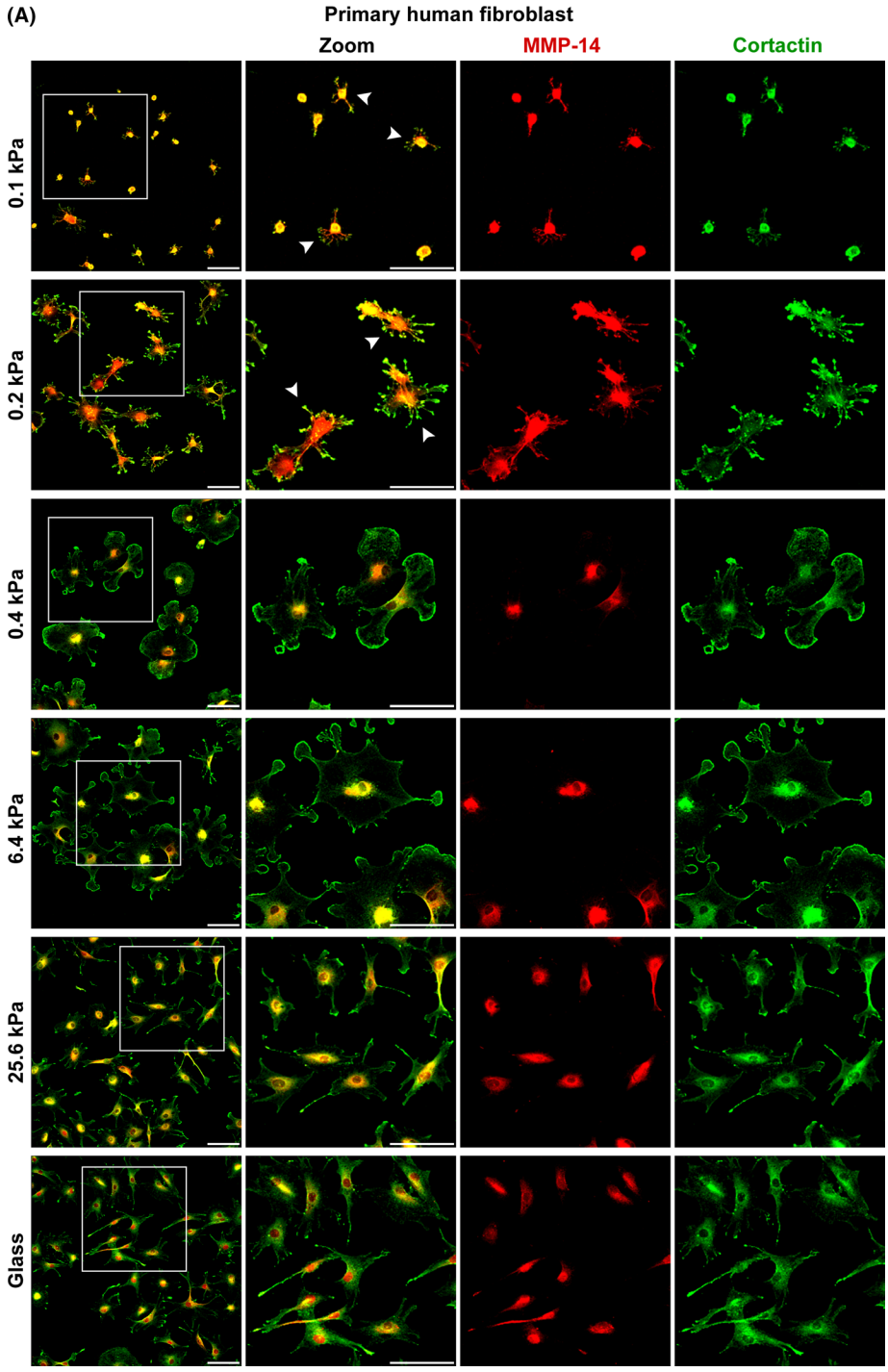

FIGURE 7: ECM softness differentially induces spontaneous ILP formation in primary cells, cancer cells, fibrosarcoma cells, and so on. Primary human fibroblasts (A) and MDA-MB-231 human breast cancer cells (B) were seeded onto gels of varying stiffness and cultured for 4 h. Invadosome marker proteins MMP-14 and cortactin were stained by primary antibodies and followed by fluorescent secondary antibodies. Arrowheads point to cells forming ILPs. Scale bar, 100 μm (A), 50 μm (B). Continues

normal and malignant cells studied here always formed more ILPs on soft substrates than on stiff substrates. These findings suggest that normal human primary fibroblasts and some cancer cells favor "softness" rather than stiffness for directional invasion, although, given the great heterogeneity of cancer cells, other cancer cells might favor "stiffness" for invasion (Alexander *et al.*, 2008). Solid tumors are believed to be stiffer than their surrounding soft tissues (Huang and Ingber, 2005; Ng and Brugge, 2009). Hence our findings suggest that surrounding tissue softness might be a natural stimulator for tumor cell invasion out of their "stiffer" primary locations.

Together these findings reveal the striking effects of soft matrix on adherens junctions, MMPs, and ILPs, which all contribute to cell invasion.

MATERIALS AND METHODS

Cell culture

Primary human fibroblasts were recovered from human synovial tissues that were obtained after synovectomy or joint replacement surgery performed at Brigham and Women's Hospital (Boston, MA). Fibroblasts were released from synovial tissue by mincing, followed by collagenase digestion, purified by serial passage as previously described (Agarwal *et al.*, 2008), and used in experiments between passages 5 and 10. Hs27 human skin fibroblasts, LL 24 human lung fibroblasts, HUV-EC-C human umbilical vein endothelial cells, MDA-MB-231 human breast cancer cells, BT549 human breast cancer cells, HS 93.T human fibrosarcoma cells, and HS 913T human fibrosarcoma cells were purchased from the American Type Culture Collection (Manassas, VA). All cells were cultured in DMEM, supplemented with 10% fetal bovine serum (FBS; Hyclone, Logan, UT), L-glutamine, penicillin/streptomycin, 2-mercaptoethanol, and essential and nonessential amino acids at 37°C under 10% CO_2 unless otherwise indicated. HUV-EC-C human umbilical vein endothelial cells were cultured in ATCC-formulated F-12K medium, supplemented with 10% FBS (Hyclone), 0.1 mg/ml heparin (Sigma-Aldrich, St. Louis, MO), 0.03–0.05 mg/ml endothelial cell growth supplement (Sigma-Aldrich), and L-glutamine, penicillin/streptomycin at 37°C under 5% CO_2. Cell culture reagents were purchased from Invitrogen (Carlsbad, CA) unless otherwise indicated.

Reagents

TIMP1, TIMP2, and batimastat were from Sigma-Aldrich. Rabbit anti-MMP14 (hinge region) and mouse anti–integrin β1 antibodies were from Abcam (Cambridge, MA). Mouse anti-cortactin antibody was from Millipore (Billerica, MA). Rabbit anti–p-c-Src (Tyr-419) antibody and Src family kinase inhibitors Dasatinib and SU6656 were from Santa Cruz Biotechnology (Santa Cruz, CA). DQ collagen, Oregon Green 488–conjugated gelatin, mouse anti–cadherin-11, mouse anti–α-catenin, and mouse anti–β-catenin antibodies, Alexa Fluor–conjugated anti-mouse, anti-rat, and anti-rabbit secondary antibodies,

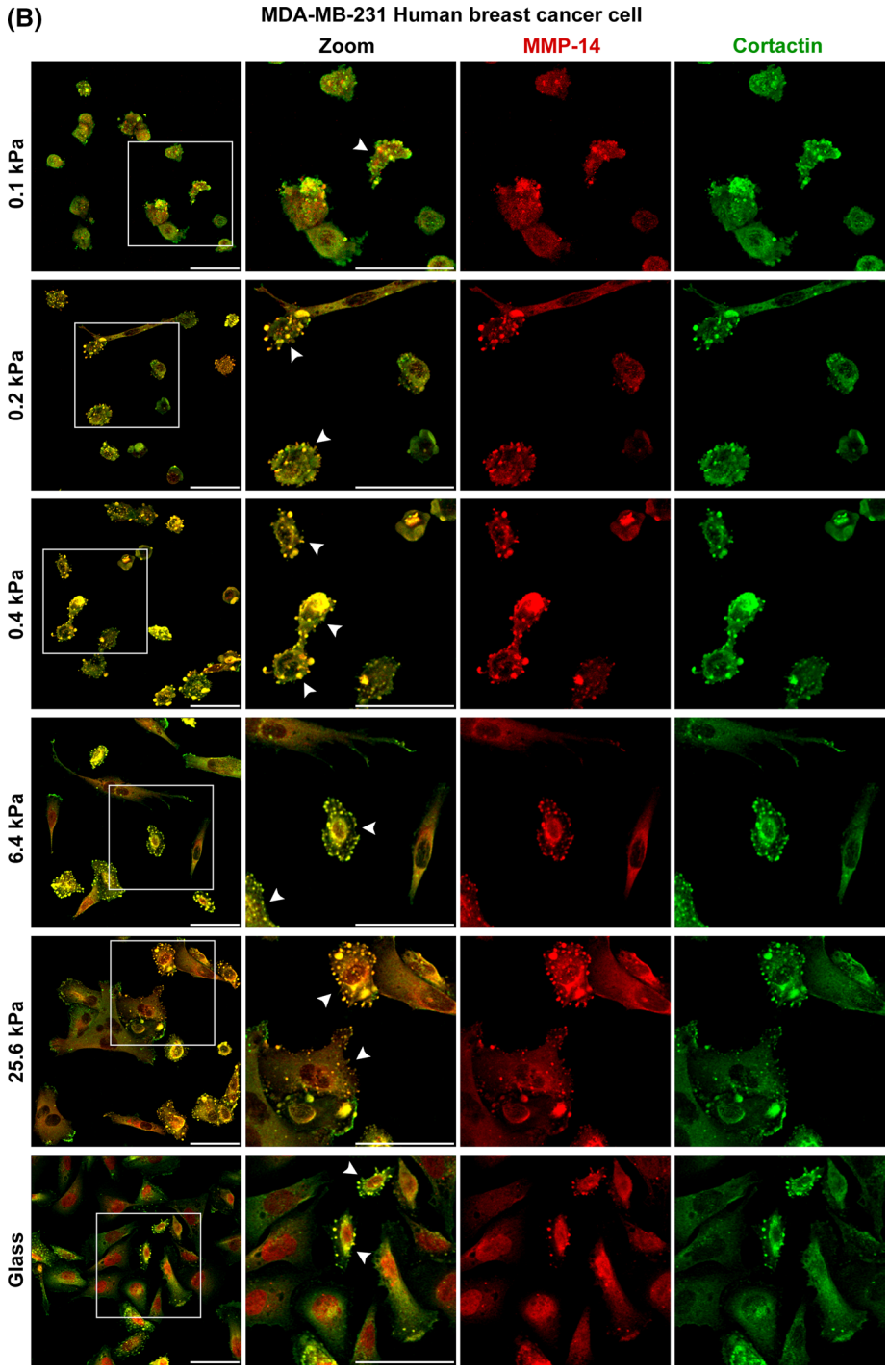

Continued

and Alexa Fluor–conjugated phalloidin were from Invitrogen. Mouse anti–p120-catenin antibody was from BD Biosciences (San Jose, CA). Mouse anti–cadherin-11 (3H10) was previously raised in this laboratory (Valencia *et al.*, 2004). DRAQ5 was from Cell Signaling (Danvers, MA). Human phosphokinase antibody array was from R&D Systems (Minneapolis, MN).

Stiffness gel preparation

Stiffness gels were prepared as previously described with slight modifications (Liu *et al.*, 2010). Briefly, round 18-mm glass coverslips (Fisher Scientific, Pittsburgh, PA) were treated with a 1% solution of 3-(trimethoxysilyl)propyl methacrylate (Sigma-Aldrich) in acetone for 30 min, followed by a brief wash in methanol, and were then completely dried. Gel solutions (100 µl/gel) containing 0.075% ammonium persulfate, 0.15% tetramethylethylenediamine, and variable ratios of acrylamide/bisacrylamide (Bio-Rad, Hercules, CA) were delivered onto the silanized coverslips. Another piece of untreated glass coverslip was placed on top of the gel solution to sandwich the polymerizing gel solutions between the two glass surfaces. After gel polymerization, the untreated glass coverslip on top was removed, and the gel with the bottom silanized coverslip was loaded into 12-well plates. Gel surface was derivatized with heterobifunctional crosslinker Sulfo-SANPAH (Fisher Scientific; Pelham and Wang, 1997). Monomeric collagen (PureCol; Advanced BioMatrix, Poway, CA), DQ collagen (Invitrogen), or Fibronectin (Invitrogen) diluted in phosphate-buffered saline (PBS) at 0.1 mg/ml was delivered to each well and incubated for 4 h at room temperature. Default coating for all experiments is PureCol unless noted otherwise. The well plate was rinsed in PBS and ultraviolet sterilized before cell seeding.

Total MMP quantity assay and total MMP activity assay

Total MMP protein quantity in cell culture conditioned media was determined and quantified by the RayBio Human MMP Array 1 (AAH-MMP-1–8; RayBiotech, Norcross, GA) according to manufacturer's instructions. Total MMP activity in cell culture conditioned media was determined using the Mca-PLGL-Dpa-AR-NH2 fluorogenic peptide substrate (ES001; R&D Systems) according to manufacturer's instructions. A 75-µl amount of conditioned medium was transferred to a single well of a 96-well plate containing 25 µl of 20 µM substrate and incubated for 30 min. Fluorescence was measured at excitation 320 nm and emission 420 nm, and background fluorescence (blank media) was subtracted for quantification. Activated recombinant human MMP-2 (902-MP; R&D Systems) was used as positive control.

Immunofluorescence microscopy and 3D directional invasion assay

For immunofluorescence staining, cells cultured on stiffness gels were fixed in 4% paraformaldehyde (Electron Microscopy Sciences, Hatfield, PA) for 15 min. For intracellular protein staining, cells were permeabilized with 0.3% Triton X-100 (Thermo Fisher Scientific, Rockford, IL) for 10 min. Permeabilized cells were labeled with

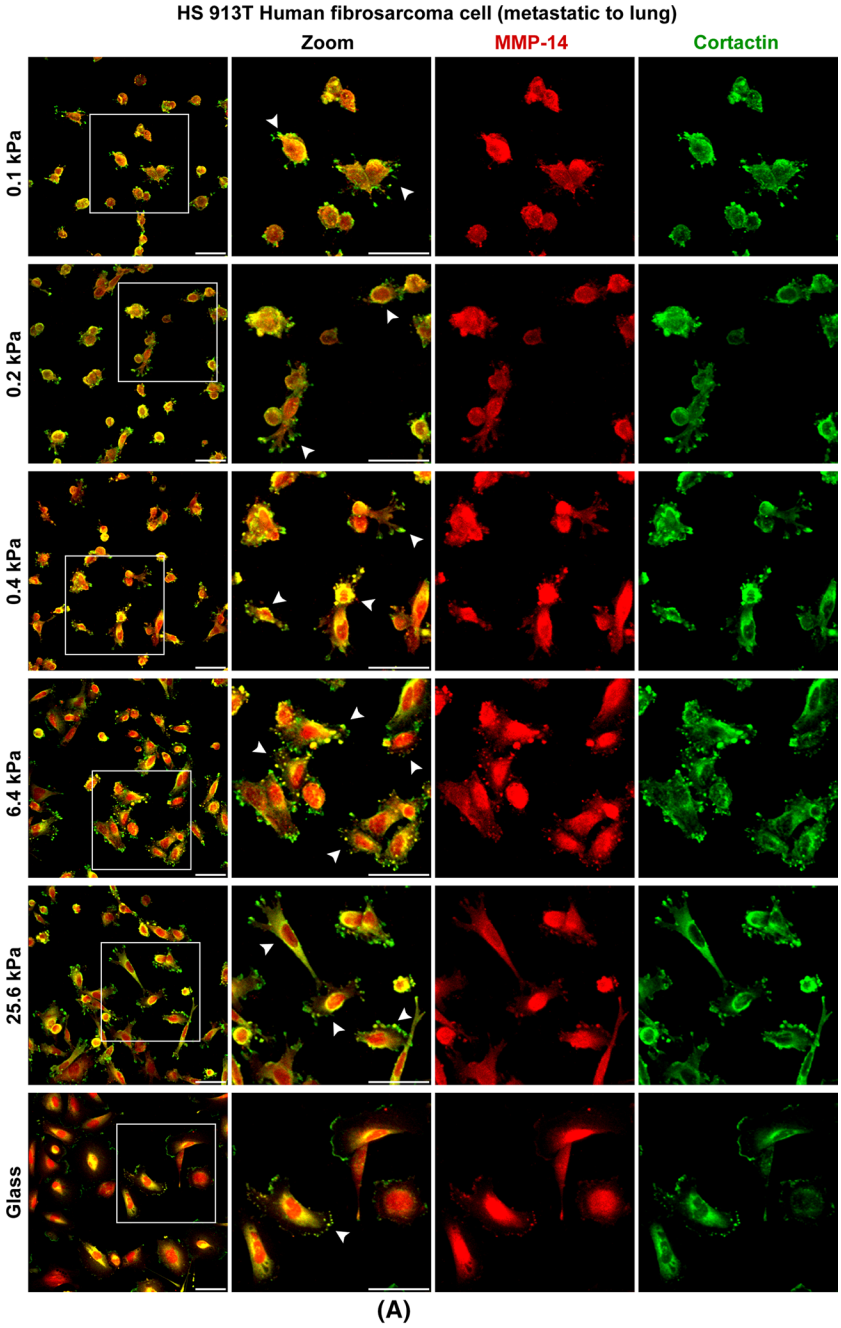

(A)

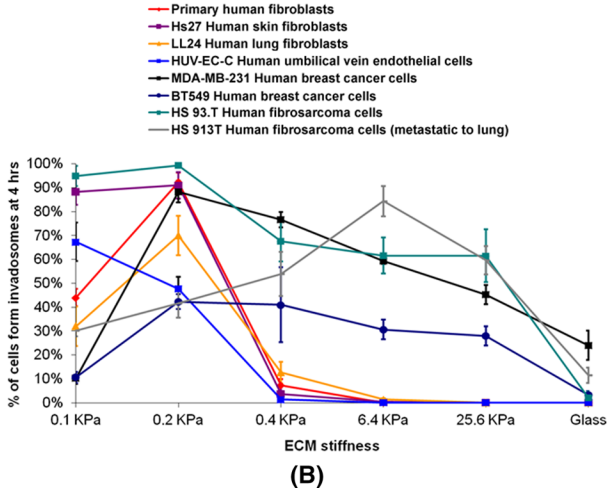

(B)

primary antibodies for 1 h at room temperature or 16 h at 4°C, followed by secondary antibody labeling for 1 h, and mounted on slides with FluorSave Reagent (Calbiochem, San Diego, CA). Immunofluorescence images were captured on a Nikon TE2000-U inverted microscope equipped with Nikon C1 confocal system controlled by Nikon EZ-C1 software, using a Nikon Plan Apo 60×/1.40 oil objective or a Nikon Plan Apo 20×/0.75 objective (Nikon, Melville, NY). The 3D confocal microscopy was performed by scanning multiple confocal layers along the *z*-axis. For 4D time-lapse confocal live-cell imaging experiments, cells were live stained by DiI (Invitrogen, Carlsbad, CA) and then seeded in 35-mm glass-bottomed Petri dishes (World Precision Instruments, Sarasota, FL) with a Matrigel dam (Supplemental Figure S2f). These dishes were mounted onto the confocal microscope with a heating chamber at 37°C and superfused with 10% CO_2. The 4D confocal microscopy was performed by 3D confocal microscopy scanning over time. Fluorescence 3D or 4D image reconstruction and protein colocalization analysis were performed in MetaMorph Imaging software, version 7.6.1.0 (Universal Imaging, Chesterfield, PA).

SDS–PAGE and Western blotting

For SDS–PAGE experiments, cells were lysed at 4°C in a cell lysis buffer of the following composition: 1% Triton X-100, 50 mM 4-(2-hydroxyethyl)-1-piperazineethanesulfonic acid, 150 mM NaCl, 5 mM EDTA, 5 mM ethylene glycol tetraacetic acid, 20 mM NaF, 20 mM sodium pyrophosphate, 1 mM phenylmethylsulfonyl fluoride, and 1 mM Na_3VO_4; pH 7.4. DC protein assays (Bio-Rad Laboratories, Hercules, CA) were performed on cell lysate samples. Equal amounts of protein from each sample were run on each lane of SDS–PAGE gels. After gel electrophoresis, proteins were transferred to a polyvinylidene fluoride membrane for Western blotting analysis. Proteins on the membranes were labeled with primary antibodies overnight at 4°C, then labeled by peroxidase-conjugated secondary antibodies and visualized by enhanced chemiluminescence detection reagents (Thermo Fisher Scientific). β-Actin was blotted as protein loading control.

Statistics

Numerical data are presented as means ± SD. Student's *t* test was used for the comparison of two means (*$p < 0.05$ considered significant).

FIGURE 8: ECM softness differentially induces spontaneous ILP formation in primary cells, cancer cells, fibrosarcoma cells, and so on. (A) HS 93.T human fibrosarcoma cells were prepared as in Figure 7. Arrowheads point to cells forming ILPs. Scale bar, 100 μm. (B) Cells as indicated were seeded onto gels of varying stiffness and cultured for 4 h. Percentage of cells forming ILPs was quantified ($n = 3$, ±SD). In each experiment, 200 cells in total were counted.

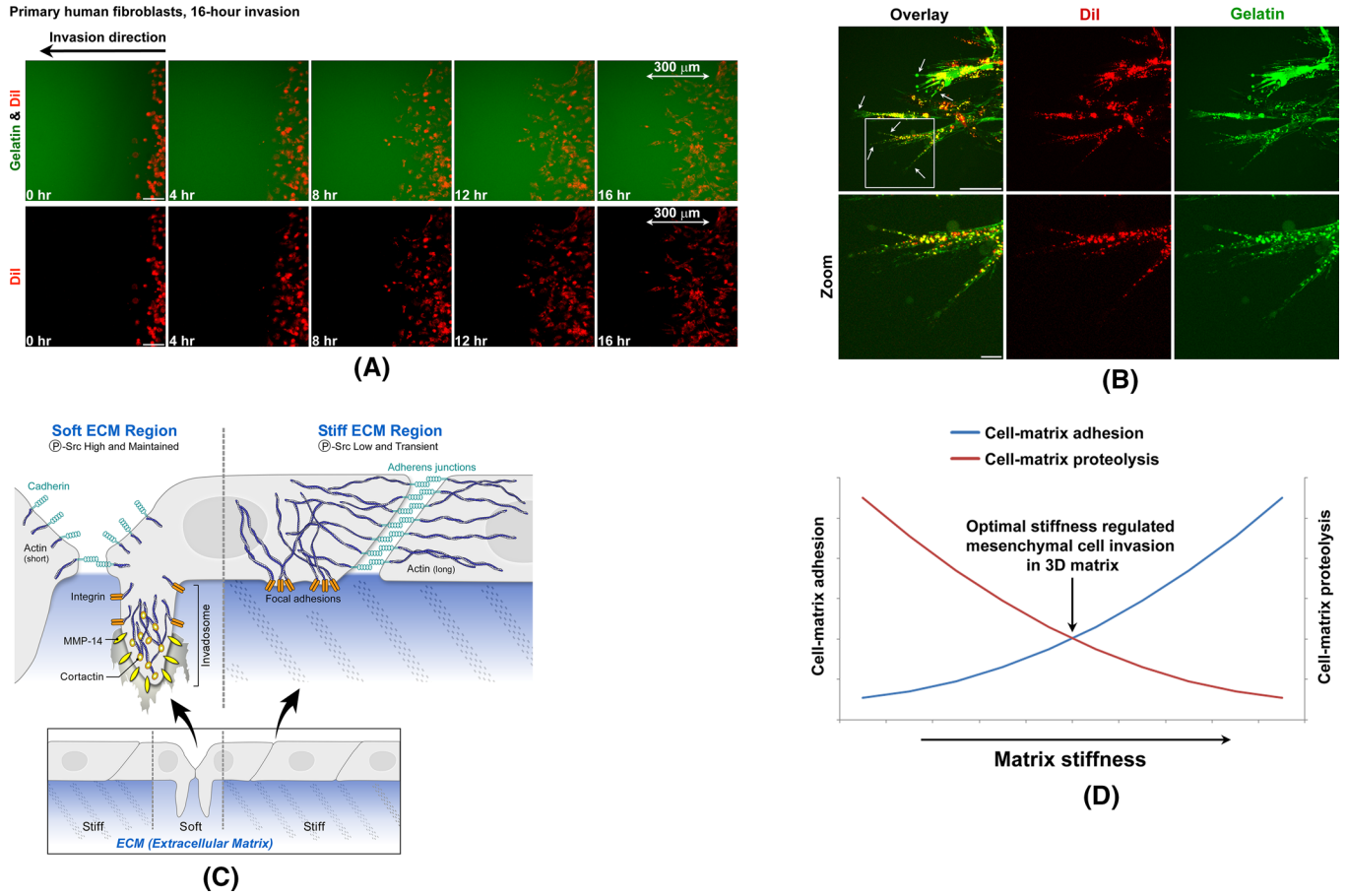

FIGURE 9: Similar ILP formation is detected in cells cultured in soft 3D matrices. (A) Primary human fibroblasts were live stained by DiI and then seeded into the 3D cell invasion assay as in Supplemental Figure S5. All 2D images were projected from relevant confocal 3D stacks by maximum projection method. Scale bar, 100 μm. Images were taken by a 20× objective with large pinhole. (B) Cells invading as in A were imaged by a 63× objective with small pinhole. All 2D images were projected from relevant confocal 3D stacks by maximum projection method. Scale bar, 100 μm. Arrows point at ILPs. (C) Schematics of ECM softness–induced ILP formation. (D) Schematics of stiffness cell-matrix adhesion curve and stiffness cell-matrix proteolysis curve.

ACKNOWLEDGMENTS

This work was supported by National Institute of Health Grants R01AR048114 and R01AR057382.

REFERENCES

Agarwal SK, Lee DM, Kiener HP, Brenner MB (2008). Coexpression of two mesenchymal cadherins, cadherin 11 and N-cadherin, on murine fibroblast-like synoviocytes. Arthritis Rheum 58, 1044–1054.

Alexander NR, Branch KM, Parekh A, Clark ES, Iwueke IC, Guelcher SA, Weaver AM (2008). Extracellular matrix rigidity promotes invadopodia activity. Curr Biol 18, 1295–1299.

Ayala I, Baldassarre M, Giacchetti G, Caldieri G, Tete S, Luini A, Buccione R (2008). Multiple regulatory inputs converge on cortactin to control invadopodia biogenesis and extracellular matrix degradation. J Cell Sci 121, 369–378.

Badowski C, Pawlak G, Grichine A, Chabadel A, Oddou C, Jurdic P, Pfaff M, Albiges-Rizo C, Block MR (2008). Paxillin phosphorylation controls invadopodia/podosomes spatiotemporal organization. Mol Biol Cell 19, 633–645.

Bharti S *et al.* (2007). Src-dependent phosphorylation of ASAP1 regulates podosomes. Mol Cell Biol 27, 8271–8283.

Bhowmick NA, Neilson EG, Moses HL (2004). Stromal fibroblasts in cancer initiation and progression. Nature 432, 332–337.

Buccione R, Orth JD, McNiven MA (2004). Foot and mouth: podosomes, invadopodia and circular dorsal ruffles. Nat Rev Mol Cell Biol 5, 647–657.

Buschman MD, Bromann PA, Cejudo-Martin P, Wen F, Pass I, Courtneidge SA (2009). The novel adaptor protein Tks4 (SH3PXD2B) is required for functional podosome formation. Mol Biol Cell 20, 1302–1311.

Carman CV (2009). Mechanisms for transcellular diapedesis: probing and pathfinding by "invadosome-like protrusions." J Cell Sci 122, 3025–3035.

Chan KT, Cortesio CL, Huttenlocher A (2009). FAK alters invadopodia and focal adhesion composition and dynamics to regulate breast cancer invasion. J Cell Biol 185, 357–370.

Diaz B, Shani G, Pass I, Anderson D, Quintavalle M, Courtneidge SA (2009). Tks5-dependent, nox-mediated generation of reactive oxygen species is necessary for invadopodia formation. Sci Signal 2, ra53.

Discher DE, Janmey P, Wang YL (2005). Tissue cells feel and respond to the stiffness of their substrate. Science 310, 1139–1143.

Duong LT, Lakkakorpi PT, Nakamura I, Machwate M, Nagy RM, Rodan GA (1998). PYK2 in osteoclasts is an adhesion kinase, localized in the sealing zone, activated by ligation of alpha(v)beta3 integrin, and phosphorylated by src kinase. J Clin Invest 102, 881–892.

Enomoto M *et al.* (2009). Autonomous regulation of osteosarcoma cell invasiveness by Wnt5a/Ror2 signaling. Oncogene 28, 3197–3208.

Friedl P, Alexander S (2011). Cancer invasion and the microenvironment: plasticity and reciprocity. Cell 147, 992–1009.

Friedl P, Borgmann S, Brocker EB (2001). Amoeboid leukocyte crawling through extracellular matrix: lessons from the *Dictyostelium* paradigm of cell movement. J Leukoc Biol 70, 491–509.

Furmaniak-Kazmierczak E, Crawley SW, Carter RL, Maurice DH, Cote GP (2007). Formation of extracellular matrix-digesting invadopodia by primary aortic smooth muscle cells. Circ Res 100, 1328–1336.

Gaggioli C, Hooper S, Hidalgo-Carcedo C, Grosse R, Marshall JF, Harrington K, Sahai E (2007). Fibroblast-led collective invasion of carcinoma cells with differing roles for RhoGTPases in leading and following cells. Nat Cell Biol 9, 1392–1400.
Gianni D, Diaz B, Taulet N, Fowler B, Courtneidge SA, Bokoch GM (2009). Novel p47(phox)-related organizers regulate localized NADPH oxidase 1 (Nox1) activity. Sci Signal 2, ra54.
Gil-Henn H *et al.* (2007). Defective microtubule-dependent podosome organization in osteoclasts leads to increased bone density in Pyk2(-/-) mice. J Cell Biol 178, 1053–1064.
Gu Z, Noss EH, Hsu VW, Brenner MB (2011). Integrins traffic rapidly via circular dorsal ruffles and macropinocytosis during stimulated cell migration. J Cell Biol 193, 61–70.
Hauck CR, Hsia DA, Ilic D, Schlaepfer DD (2002). v-Src SH3-enhanced interaction with focal adhesion kinase at beta 1 integrin-containing invadopodia promotes cell invasion. J Biol Chem 277, 12487–12490.
Hinz B (2007). Formation and function of the myofibroblast during tissue repair. J Invest Dermatol 127, 526–537.
Huang S, Ingber DE (2005). Cell tension, matrix mechanics, and cancer development. Cancer Cell 8, 175–176.
Janmey PA, McCulloch CA (2007). Cell mechanics: integrating cell responses to mechanical stimuli. Annu Rev Biomed Eng 9, 1–34.
Jiang G, den Hertog J, Su J, Noel J, Sap J, Hunter T (1999). Dimerization inhibits the activity of receptor-like protein-tyrosine phosphatase-alpha. Nature 401, 606–610.
Jodele S, Blavier L, Yoon JM, DeClerck YA (2006). Modifying the soil to affect the seed: role of stromal-derived matrix metalloproteinases in cancer progression. Cancer Metastasis Rev 25, 35–43.
Kessenbrock K, Plaks V, Werb Z (2010). Matrix metalloproteinases: regulators of the tumor microenvironment. Cell 141, 52–67.
Lammermann T, Sixt M (2009). Mechanical modes of "amoeboid" cell migration. Curr Opin Cell Biol 21, 636–644.
Lee DM, Kiener HP, Agarwal SK, Noss EH, Watts GF, Chisaka O, Takeichi M, Brenner MB (2007). Cadherin-11 in synovial lining formation and pathology in arthritis. Science 315, 1006–1010.
Levental KR *et al.* (2009). Matrix crosslinking forces tumor progression by enhancing integrin signaling. Cell 139, 891–906.
Linder S (2009). Invadosomes at a glance. J Cell Sci 122, 3009–3013.
Liu F, Mih JD, Shea BS, Kho AT, Sharif AS, Tager AM, Tschumperlin DJ (2010). Feedback amplification of fibrosis through matrix stiffening and COX-2 suppression. J Cell Biol 190, 693–706.
Lorentzen A, Bamber J, Sadok A, Elson-Schwab I, Marshall CJ (2011). An ezrin-rich, rigid uropod-like structure directs movement of amoeboid blebbing cells. J Cell Sci 124, 1256–1267.
Magalhaes MA, Larson DR, Mader CC, Bravo-Cordero JJ, Gil-Henn H, Oser M, Chen X, Koleske AJ, Condeelis J (2011). Cortactin phosphorylation regulates cell invasion through a pH-dependent pathway. J Cell Biol 195, 903–920.
Mizutani K, Miki H, He H, Maruta H, Takenawa T (2002). Essential role of neural Wiskott-Aldrich syndrome protein in podosome formation and degradation of extracellular matrix in src-transformed fibroblasts. Cancer Res 62, 669–674.
Murphy DA, Courtneidge SA (2011). The "ins" and "outs" of podosomes and invadopodia: characteristics, formation and function. Nat Rev Mol Cell Biol 12, 413–426.
Myers KA, Applegate KT, Danuser G, Fischer RS, Waterman CM (2011). Distinct ECM mechanosensing pathways regulate microtubule dynamics to control endothelial cell branching morphogenesis. J Cell Biol 192, 321–334.
Nada S, Okada M, MacAuley A, Cooper JA, Nakagawa H (1991). Cloning of a complementary DNA for a protein-tyrosine kinase that specifically phosphorylates a negative regulatory site of p60c-src. Nature 351, 69–72.
Nagase H, Visse R, Murphy G (2006). Structure and function of matrix metalloproteinases and TIMPs. Cardiovasc Res 69, 562–573.
Neilson EG (2006). Mechanisms of disease: fibroblasts—a new look at an old problem. Nat Clin Pract Nephrol 2, 101–108.
Nelson CM, Vanduijn MM, Inman JL, Fletcher DA, Bissell MJ (2006). Tissue geometry determines sites of mammary branching morphogenesis in organotypic cultures. Science 314, 298–300.
Ng MR, Brugge JS (2009). A stiff blow from the stroma: collagen crosslinking drives tumor progression. Cancer Cell 16, 455–457.
Oneyama C, Hikita T, Enya K, Dobenecker MW, Saito K, Nada S, Tarakhovsky A, Okada M (2008). The lipid raft-anchored adaptor protein Cbp controls the oncogenic potential of c-Src. Mol Cell 30, 426–436.
Parekh A, Ruppender NS, Branch KM, Sewell-Loftin MK, Lin J, Boyer PD, Candiello JE, Merryman WD, Guelcher SA, Weaver AM (2011). Sensing and modulation of invadopodia across a wide range of rigidities. Biophys J 100, 573–582.
Parsons JT, Parsons SJ (1997). Src family protein tyrosine kinases: cooperating with growth factor and adhesion signaling pathways. Curr Opin Cell Biol 9, 187–192.
Pathak A, Kumar S (2012). Independent regulation of tumor cell migration by matrix stiffness and confinement. Proc Natl Acad Sci USA 109, 10334–10339.
Pelham RJ Jr, Wang Y (1997). Cell locomotion and focal adhesions are regulated by substrate flexibility. Proc Natl Acad Sci USA 94, 13661–13665.
Pignatelli J, Tumbarello DA, Schmidt RP, Turner CE (2012). Hic-5 promotes invadopodia formation and invasion during TGF-beta-induced epithelial-mesenchymal transition. J Cell Biol 197, 421–437.
Poincloux R, Collin O, Lizarraga F, Romao M, Debray M, Piel M, Chavrier P (2011). Contractility of the cell rear drives invasion of breast tumor cells in 3D Matrigel. Proc Natl Acad Sci USA 108, 1943–1948.
Sabeh F, Li XY, Saunders TL, Rowe RG, Weiss SJ (2009). Secreted versus membrane-anchored collagenases: relative roles in fibroblast-dependent collagenolysis and invasion. J Biol Chem 284, 23001–23011.
Schwartz MA, Schaller MD, Ginsberg MH (1995). Integrins: emerging paradigms of signal transduction. Annu Rev Cell Dev Biol 11, 549–599.
Shibue T, Brooks MW, Inan MF, Reinhardt F, Weinberg RA (2012). The outgrowth of micrometastases is enabled by the formation of filopodium-like protrusions. Cancer Discov 2, 706–721.
Superti-Furga G, Fumagalli S, Koegl M, Courtneidge SA, Draetta G (1993). Csk inhibition of c-Src activity requires both the SH2 and SH3 domains of Src. EMBO J 12, 2625–2634.
Valencia X *et al.* (2004). Cadherin-11 provides specific cellular adhesion between fibroblast-like synoviocytes. J Exp Med 200, 1673–1679.
Wang HB, Dembo M, Wang YL (2000). Substrate flexibility regulates growth and apoptosis of normal but not transformed cells. Am J Physiol Cell Physiol 279, C1345–C1350.
Williams KC, Coppolino MG (2011). Phosphorylation of membrane type 1-matrix metalloproteinase (MT1-MMP) and its vesicle-associated membrane protein 7 (VAMP7)-dependent trafficking facilitate cell invasion and migration. J Biol Chem 286, 43405–43416.
Wolf K, Friedl P (2011). Extracellular matrix determinants of proteolytic and non-proteolytic cell migration. Trends Cell Biol 21, 736–744.
Wolf K, Wu YI, Liu Y, Geiger J, Tam E, Overall C, Stack MS, Friedl P (2007). Multi-step pericellular proteolysis controls the transition from individual to collective cancer cell invasion. Nat Cell Biol 9, 893–904.
Yamaguchi H *et al.* (2005). Molecular mechanisms of invadopodium formation: the role of the N-WASP-Arp2/3 complex pathway and cofilin. J Cell Biol 168, 441–452.
Yamaguchi H, Yoshida S, Muroi E, Yoshida N, Kawamura M, Kouchi Z, Nakamura Y, Sakai R, Fukami K (2011). Phosphoinositide 3-kinase signaling pathway mediated by p110alpha regulates invadopodia formation. J Cell Biol 193, 1275–1288.
Zachary I, Rozengurt E (1992). Focal adhesion kinase (p125FAK): a point of convergence in the action of neuropeptides, integrins, and oncogenes. Cell 71, 891–894.
Zaman MH, Trapani LM, Sieminski AL, Mackellar D, Gong H, Kamm RD, Wells A, Lauffenburger DA, Matsudaira P (2006). Migration of tumor cells in 3D matrices is governed by matrix stiffness along with cell-matrix adhesion and proteolysis. Proc Natl Acad Sci USA 103, 10889–10894.